

Nonlocal control of spin-spin correlations in a finite-geometry helical edge

Sonu Verma and Arijit Kundu

Department of Physics, Indian Institute of Technology Kanpur, Kanpur 208016, India



(Received 3 June 2018; revised manuscript received 15 August 2018; published 27 March 2019)

An infinite edge of a quantum Hall system prohibits indirect exchange coupling between two spins, whereas a quantum spin-Hall edge prohibits out-of-plane coupling. In this study, we analyze an unexpected breakdown of this behavior in a finite system, where the two spins can interact also via a longer path that traverses the whole perimeter of the system. We explain this using an analytical model as well as tight-binding models in real space. Based on this finding, we show how using a lead far away from the spins can switch the coupling on and off among them nonlocally.

DOI: [10.1103/PhysRevB.99.121409](https://doi.org/10.1103/PhysRevB.99.121409)

Introduction. Nonlocal control of the interaction among spins has been a field of intense study in the past few years, and it has assisted in quantum-information processing [1] as well as spintronic applications. Effective interaction among localized spins mediated by the underlying delocalized electrons is described by the Ruderman-Kittel-Kasuya-Yoshida (RKKY) theory [2]. It has been proposed to control such coupling nonlocally, such as via optical means [3,4], an external magnetic field [5], or an applied electric field [6,7], among others methods [8–15], and some of these approaches have been verified experimentally [16–19]. Solid-state-based systems, spin-orbit coupled systems [20–22], and especially topological systems are among the significant candidates that can mediate long-range controllable coupling [6,23–27] among spins.

Quantum Hall (QH) and quantum spin-Hall (QSH) states are characterized by nonzero spin-Chern numbers and they have topologically protected *chiral* edge states, where a given spin mode can traverse in a given direction [28]. QH states break time-reversal symmetry and have edge states where both spins move in chiral channels in the same direction, whereas in QSH states, the edge states have oppositely moving channels for opposite spins, preserving the time-reversal symmetry of the system. Due to the chiral nature of states and the one-dimensionality, it is expected that such edge states would carry long-range correlation also among two spins placed on the edge, which is indeed what has been explored in recent studies [23,25,29].

The spin-momentum locking (helicity) of the edge states gives rise to vanishing out-of-plane RKKY coupling for the spins on a QSH edge, whereas in a QH edge, all components of the RKKY coupling vanish [23,25]. In this work, we analyze and propose manipulating an unexpected breakdown of this result when the geometry is finite. This behavior is a result of the fact that in a finite geometry, the helical edge states can come back by traversing the whole edge of the sample. Further, such long-range coupling between the spins is found to be antiferromagnetic in nature, and the amplitude of the coupling becomes almost independent of the distance between the spins. We show this using a lattice simulation

with two models, one in a hexagonal lattice [30,31] and the other in a square lattice [32]. This surprising behavior can also be explained using an analytical model of the edge states. The longer path of interaction between the spins through the whole perimeter of the system can be controlled by using a lead attached to the edge far away from the spins, which can induce decoherence in the edge states, resulting in turning off the relevant interaction among the spins. This mechanism allows us to have a truly nonlocal control of the coupling between the spins, where none of the local parameters are modified.

RKKY interaction by an infinite chiral edge. The hallmark of topologically nontrivial states are the chiral edge states where a given spin can move in a definite direction. In particular, the helical edge (running along the $\pm x$ direction) of the QSH phase can be represented by the Hamiltonian $H_{\text{edge}} = -iv_F \sigma_z \partial_x$, where σ_i are the Pauli matrices of the spin and v_F is the Fermi velocity. The corresponding Green's function is block-diagonal in the up and down spin sector [23]:

$$G_{\pm}^{\text{QSH}}(x, x'; \omega) = -\frac{i}{v_F} e^{i\frac{\omega}{v_F}(x-x')} \theta(\pm(x-x')), \quad (1)$$

where the \pm refers to up and down spin states, respectively.

Spin-susceptibility of a system can be captured by the effective interaction between two impurity spins, mediated by conduction electrons of the system. Considering that the impurity spins ($\mathbf{S}_1, \mathbf{S}_2$ at positions x_1, x_2 on the edge) couple to the delocalized electrons in the edge through the Kondo coupling $H' = -\frac{J}{2} \sum_{r,\sigma,\sigma'} \psi_{r\sigma}^\dagger(x) [S_{1,\sigma\sigma'} \delta(x-x_1) + S_{2,\sigma\sigma'} \delta(x-x_2)] \psi_{r\sigma}(x)$, where r could denote left- or right-moving states, second-order perturbation in H' gives the effective RKKY interaction among the impurity spins,

$$H_{\text{RKKY}} = -\frac{J^2}{\pi} \int_{-\infty}^{E_F} d\omega \text{Tr}[(\mathbf{S}_1 \cdot \boldsymbol{\sigma}) G(\mathbf{r}_{12}; \omega + i0+) (\mathbf{S}_2 \cdot \boldsymbol{\sigma}) \times G(-\mathbf{r}_{12}; \omega + i0+)] \quad (2)$$

$$\equiv \sum_{i,j=x,y,z} \mathcal{J}_{ij} S_{1i} S_{2j}, \quad (3)$$

where \mathbf{r}_{12} is the separation of the two spins, and the resultant \mathcal{J}_{ij} forms the spin-spin correlation matrix.

Equation (1) immediately results in vanishing *Ising* interaction among spins that are aligned as up and down spins, i.e., $\mathcal{J}_{zz} = 0$. The appearance of the θ functions in Eq. (1) is essentially responsible for this behavior, which dictates that $|G_{\sigma\sigma}(x, x'; \omega)|$ is nonvanishing only for $x - x' >$ and < 0 for up and down spin modes respectively. A similar argument follows for a QH phase, and as both spins can move in only one direction, the argument of the θ function in Eq. (1) has the same sign, which results in all correlations \mathcal{J}_{ij} vanishing in a QH edge.

Lattice simulation. To study a finite topological system, below we consider a Hamiltonian in a hexagonal lattice that can represent QH, QSH, or a normal insulator for different ranges of parameters. Another model on a square lattice has also been studied and is detailed in the supplemental material [40]. The Hamiltonian on the hexagonal lattice is [30,31]

$$H = -t \sum_{\langle i,j \rangle, \sigma} c_{i\sigma}^\dagger c_{j\sigma} + \sum_{\langle\langle i,j \rangle\rangle, \sigma} i\lambda_\sigma v_{ij} c_{i\sigma}^\dagger c_{j\sigma} + \sum_{i\sigma} \Delta_i c_{i\sigma}^\dagger c_{i\sigma}, \quad (4)$$

where $c_{i\sigma}^\dagger$ is the electronic creation operator at site i with spin $\sigma = \pm$ for up and down spin electrons, respectively. t is the nearest-neighbor hopping, which also serves as our unit of energy. Next to the nearest-neighbor hopping amplitude, λ_σ , is the spin-orbit coupling strength. $\Delta_i = \mu \pm \Delta$ contains the chemical potential μ , which we keep at zero, and the staggered potential Δ , where \pm applies to A and B sublattices. v_{ij} is ± 1 depending on clockwise or anticlockwise hopping. This Hamiltonian can be realized in various solid-state systems such as silicene, germanene, and stanene [33,34]. When $\lambda_\sigma = \sigma\lambda$, the Hamiltonian is time-reversal symmetric, and the ground state is a QSH state when $\lambda > \Delta$. If $\lambda_\sigma = \lambda$, i.e., spin-independent, then the ground state represents a QH state when $\lambda > \Delta$. In what follows, it is not required to have a finite Δ , but typically it helps in maintaining numerical stability. In passing we note that time-reversal symmetry breaking λ can be introduced through a circularly polarized irradiation on the sample [33,35,36], which can provide a way for fine-tuning the parameter. Although the viability of the application of such a system is still under investigation, application of terahertz radiation in spintronics applications is viable [3,37].

The result of the preceding section, i.e., vanishing \mathcal{J}_{zz} correlation for an infinite QSH edge, can be verified numerically, as shown in Fig. 1(a). All other terms in the correlation matrix are generally nonzero, including the off-diagonal elements, resulting in Dzyaloshinskii-Moriya interaction among the spins [23].

Instead of an infinite nanoribbon, for a finite geometry, using the Green's function $G(\omega) = [\omega - H + i0^+]^{-1}$ in real space, the RKKY interaction can be computed as second-order perturbation, Eq. (2). The impurity spins can be taken into account within H using the Kondo coupling between the localized spins, $\mathbf{S}_1, \mathbf{S}_2$, put at site i, j , and the delocalized electrons given by

$$H' = -\frac{J}{2} \sum_{\sigma\sigma'} c_{i\sigma}^\dagger S_{1,\sigma\sigma'} c_{i\sigma'} + c_{j\sigma}^\dagger S_{2,\sigma\sigma'} c_{j\sigma'}. \quad (5)$$

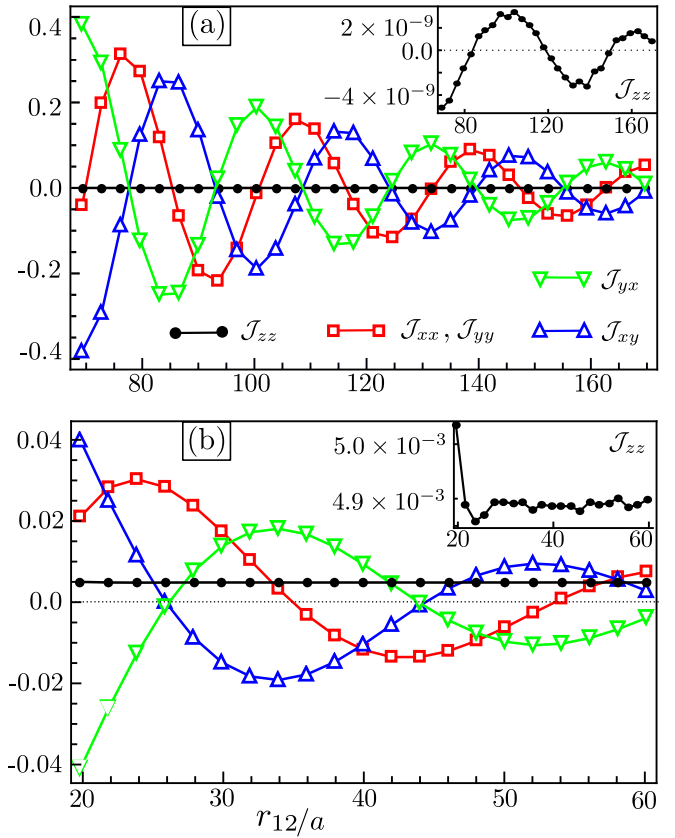


FIG. 1. (a) For an infinite nanoribbon of the QSH state, the RKKY interaction (in units of J^2) between two spins put on an edge is significantly small when the spins' moments are aligned in the up/down direction (i.e., $\mathcal{J}_{zz} \approx 0$), resulting from the chiral nature of the edges. (b) In contrast, for a finite geometry, \mathcal{J}_{zz} is finite. For numerical simulation in (a), a zigzag nanoribbon of width 16 sites has been used, whereas in (b) a system size of $N_x \times N_y = 80 \times 16$ sites has been used with the impurity spins on the longer zigzag edge. Other parameters used are $\lambda = 0.5$, $\Delta = 0.1$, and $t = 1.0$.

The RKKY interaction can also be obtained using an exact diagonalization method in a finite geometry [39]. Despite the fact that the exact diagonalization is numerically less expensive, we use the Green's function method as it provides more flexibility, especially for an open system, as we discuss later. The result from exact diagonalization matches with the second-order perturbation when J is sufficiently small [38,39].

The resulting diagonal terms of interaction matrix among the spins put on the edge of a finite QSH geometry is plotted in Fig. 1, which is markedly different from what is predicted through Eq. (1), as the interaction among the spins is nonzero even when the spins are both up or down, i.e., $\mathcal{J}_{zz} \neq 0$. As the chiral nature of the modes is still present, this breakdown from the previous result is unexpected.

To explore the reason for this, we take a simple geometry of a disk of radius R , where the chiral modes can run along the perimeter. The Hamiltonian of the 1D edge modes is then $H_{\text{edge}} = \frac{v_F \sigma_z}{R} (-i\partial_\phi + \frac{1}{2})$, ϕ being the azimuthal angle. Angular momentum $-i\partial_\phi$ is quantized with energy eigenvalues

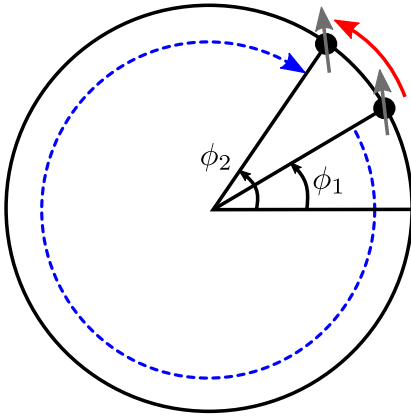


FIG. 2. For a QSH disk, the edge states run along the edge of the disk with impurity spins put in positions ϕ_1 and ϕ_2 . The spins can be connected via two paths as shown, making all relevant couplings between the spins nonvanishing.

$E_l = \sigma \frac{v_F}{R} (l + \frac{1}{2})$ [40]; with the Green's function

$$G_{\sigma\sigma}(\phi, \phi'; \omega) = \sum_l \frac{e^{i(\phi - \phi')l} / 2\pi}{R\omega + iR\eta - \sigma v_F (l + 1/2)}, \quad (6)$$

where $\sigma = \pm 1$ is for up/down spin, respectively. Note that it is not possible, in general, to convert this summation into an integral form as the integrand changes swiftly from l to $l + 1$, unless the phase ϕ is very small. In contrast to Eq. (1), this Green's function, in the limit when $\eta < v_F/2\pi R$, can now connect between arbitrary points on the circle [i.e., $|G_{\sigma\sigma}(\Delta\phi, \omega)|$ is nonzero for all $\Delta\phi = \phi - \phi'$] for both of the spin modes [40]. This essentially captures that in a finite geometry the interaction among the spins is possible through two possible paths (Fig. 2). In the second-order process, Eq. (3), it turns out that the integrand of Eq. (2) for the \mathcal{J}_{zz} component becomes independent of $\Delta\phi$, giving rise to distance-independent coupling between the spins [41]. Such a distance-independent nature is true only for the \mathcal{J}_{zz} coupling, whereas other correlation matrix elements remain functions of $\Delta\phi$. An analytical explanation is given in the supplemental material [40]. The results of Fig. 1 in light of this discussion are one of our main results.

The inversion broken nature of the QSH states also results in finite noncollinear Dzyaloshinskii-Moriya interaction among the impurity spins, which is present in either finite or infinite geometry. For the QH edge, a similar observation to QSH is made in which, instead of the vanishing correlation matrix \mathcal{J}_{ij} , one observes nonvanishing values for all of the elements. In the simple model of QH, Eq. (4), the diagonal elements of the correlation matrix become independent of the distance between the spins, whereas the off-diagonal elements remain zero.

The preceding discussion is strictly true if the perimeter of the finite QH/QSH geometry is not larger than the mean free path of the electrons at the edge states [40]. As the QH/QSH edge prohibits backscattering, one expects a large mean free path of order a few hundred nanometers [42]. The consideration of a finite mean free path would result in further decay of all the elements of the correlation matrix.

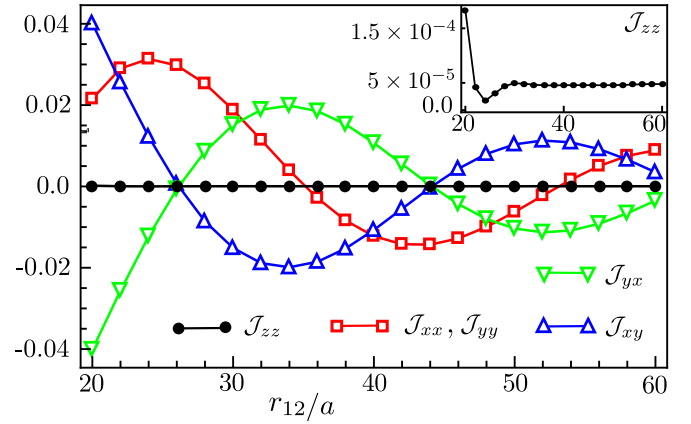


FIG. 3. Coupling strengths \mathcal{J}_{ij} (in units of J^2) for spins on the QSH edge that is connected to a lead on one side. The out-of-plane component \mathcal{J}_{zz} vanishes as the edge states suffer from the decoherence introduced by the lead. For numerical simulation, $\pi\rho t_0^2 = 0.5$ (in units of t) has been used to couple to the right side of the system, where t_0 is the system-lead coupling amplitude. Other parameters are those of Fig. 1(b).

Nonlocal control using leads. Given the different nature of interaction among spins in an infinite and finite geometry, one natural question is whether such a difference can be engineered without actually altering the geometry. Essentially prohibiting the edge states from fully traversing the perimeter should mimic the behavior of the infinite geometry, which can be achieved using a lead attached to the edge far from the two impurities. Then, for a sufficiently strong system-lead coupling, the interaction will vanish.

We proceed to treat the system with the lead attached by considering a self-energy contribution to the Green's function $G(\omega)$ of the system:

$$G(\omega)^{-1} = \omega - (H + H') - i\Sigma(\omega), \quad (7)$$

where $\Sigma(\omega) = -iK^\dagger g(\omega)K$ is the self-energy of the lead, K is the system-lead coupling matrix, and $g(\omega)$ is the lead's Green's function. The QSH edge states live within the bulk gap, and it is expected that most of the contribution in the RKKY interaction comes from states near the Fermi energy. So, without loss of generality it is sufficient to take the approximation that the lead's Green's function is independent of energy, and we write $g(\omega) \approx i\pi\rho$, where ρ is the (energy-independent) density of states of the lead at the contact. The effective Green's function can be used in Eq. (2) to compute the interaction between the spins [43].

If the lead is attached, as expected, we observe a sharp drop in the zz component of the interaction, whereas other components are effectively not affected, as shown in Fig. 3. The \mathcal{J}_{zz} drops as an exponential function of the lead's density of state, shown in Fig. 4, but the drop becomes slower after a threshold value of ρ is reached. In our simulation, we have attached the lead to the shorter side of a rectangular system that has 80×16 sites. The selective action of the lead to the Ising interaction is a direct demonstration of the helical nature of the edge states. For a QH system, such an arrangement can control the full spin-spin correlation matrix. This can provide a way to identify the helical nature of edge states by measuring

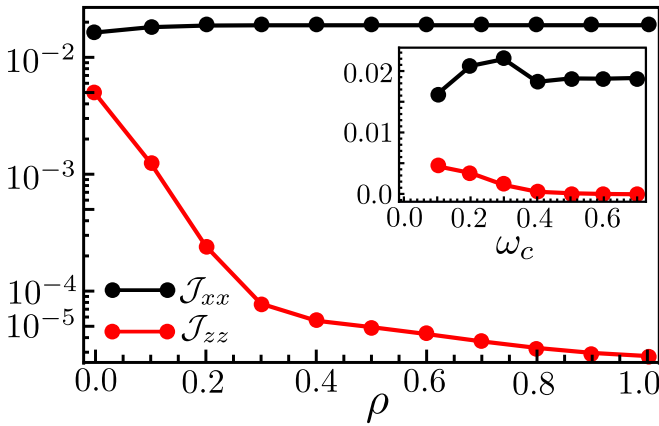


FIG. 4. With increasing density of states (ρ) of the lead, the out-of-plane correlation \mathcal{J}_{zz} (in units of J^2) vanishes whereas other coupling terms remain virtually unaffected. Inset: for a ρ that is 0.5 for $0 > \omega > \omega_c$, the \mathcal{J}_{zz} rapidly decreases as a function of ω_c until it reaches the bulk gap, which is 0.4 in our simulation. The two impurities are at (8, 16) and (30, 16), and other parameters are the same as in Fig. 1.

the spin susceptibility [44], and it can be used as an effective control of spin-spin interaction in spintronic applications. This is one of our main results.

In a realistic setup, the lead's density of states will be dependent on the energy, but our main finding should remain intact. In fact, it is sufficient to consider the lead as a quantum dot with a broadening of its level of the order of the spin-orbit gap ($\delta = \lambda - \Delta$) of the system, which is typically of the order of a few millielectron volts. We further show in Fig. 4 that as long as $\rho(\omega)$ is nonzero for the range of ω within the bulk gap of the QSH system, the \mathcal{J}_{zz} correlation remains vanishingly small, whereas as soon as $\rho(\omega)$ is zero for a range of ω where edge states exist, \mathcal{J}_{zz} acquires a finite value. This provides a concrete way to control the interaction among the spins: for turning the interaction on or off, it is sufficient to either change the quantum dot's band gap through a gate bias or the system to lead coupling.

Although unrealistic, the same result can be achieved using a finite $i\eta$ ($\eta > 0$) added on the right-hand side of the Eq. (7) instead of the lead, which would basically add a finite lifetime to *all* the eigenstates. As the states near the Fermi energy are

moving with the Fermi velocity, the coherence is present only for a given length of their path (i.e., the mean free path) given by $\sim v_F/\eta$. If the perimeter is larger than the finite length, then Ising interaction would inevitably vanish. But a finite η will effect also other possible interactions among the spins.

Discussion. The effective system size we have taken is of the order of a few nanometers (about 100 lattice spacings of typical solid-state systems). In other scales, essentially the spin-orbit coupling λ is taken to be large enough (please see the figure caption of Fig. 1) for the benefit of numerical simulation. A larger spin-orbit coupling yields a larger band gap in the bulk, although it results in smaller spin-spin correlation [40]. In realistic systems, even if the spin-orbit coupling is smaller, the system size can be much larger, so that the RKKY interaction mediated by the bulk states can still be neglected. To clearly observe the physics we propose, one needs to have a system whose perimeter is much larger than the mean free path of the bulk states, but shorter than the mean free path of the edge states. We expect the results to hold for absorbed impurities [45] as well.

Interaction in the one-dimensional edge can fractionalize the modes, and in general more than one propagating mode will be present and most of the conclusions of an infinite edge follow similarly [25]. A study with interaction is left for the future, but we expect the physics behind Fig. 2 to remain intact. In passing, we note that, interestingly, distant-independent and nonoscillating RKKY interaction has also been reported in an interacting graphene system [46], although the mechanism is different. With interaction, the graphene edges become spin-polarized, rendering antiferromagnetic orientation costly irrespective of the distance.

In summary, we theoretically demonstrate how the effective interaction among spins on a QSH or a QH edge differs in nature in a finite system compared to an infinite edge. The difference in nature can be observed using a lead attached to the system with a controllable density of states of the lead. This provides both a way to identify the helical edges of a system as well as a truly nonlocal way to control the interaction among the spins.

Acknowledgments. We would like to acknowledge useful communication with H. A. Fertig (IU Bloomington), S. Satpathy (Univ. Missouri), M. Sherafati (Truman State Univ.), and S. Mukhopadhyay (IIT Kanpur) during various parts of the work.

-
- [1] L. I. Glazman and R. C. Ashoori, *Science* **304**, 524 (2004).
 [2] M. A. Ruderman and C. Kittel, *Phys. Rev.* **96**, 99 (1954); T. Kasuya, *Prog. Theor. Phys.* **16**, 45 (1956); K. Yosida, *Phys. Rev.* **106**, 893 (1957).
 [3] U. Meyer, G. Haack, C. Groth, and X. Waintal, *Phys. Rev. Lett.* **118**, 097701 (2017).
 [4] C. Piermarocchi, P. Chen, L. J. Sham, and D. G. Steel, *Phys. Rev. Lett.* **89**, 167402 (2002).
 [5] G. Usaj, P. Lustemberg, and C. A. Balseiro, *Phys. Rev. Lett.* **94**, 036803 (2005).
 [6] Y.-W. Lee and Y.-L. Lee, *Phys. Rev. B* **91**, 214431 (2015).
 [7] N. Klier, S. Sharma, O. Pankratov, and S. Shallcross, *Phys. Rev. B* **94**, 205436 (2016).
 [8] A. V. Parafilo and M. N. Kiselev, *Phys. Rev. B* **97**, 035418 (2018).
 [9] N. Y. Yao, L. I. Glazman, E. A. Demler, M. D. Lukin, and J. D. Sau, *Phys. Rev. Lett.* **113**, 087202 (2014).
 [10] P. Simon, R. López, and Y. Oreg, *Phys. Rev. Lett.* **94**, 086602 (2005).
 [11] H. Tamura and L. Glazman, *Phys. Rev. B* **72**, 121308(R) (2005).
 [12] M. Yang and S.-S. Li, *Phys. Rev. B* **74**, 073402 (2006).

- [13] M. Friesen, A. Biswas, X. Hu, and D. Lidar, *Phys. Rev. Lett.* **98**, 230503 (2007).
- [14] J.-J. Zhu, K. Chang, R.-B. Liu, and H.-Q. Lin, *Phys. Rev. B* **81**, 113302 (2010).
- [15] D. Tutuc, B. Popescu, D. Schuh, W. Wegscheider, and R. J. Haug, *Phys. Rev. B* **83**, 241308(R) (2011).
- [16] N. J. Craig, J. M. Taylor, E. A. Lester, C. M. Marcus, M. P. Hanson, and A. C. Gossard, *Science* **304**, 565 (2004).
- [17] S. Sasaki, S. Kang, K. Kitagawa, M. Yamaguchi, S. Miyashita, T. Maruyama, H. Tamura, T. Akazaki, Y. Hirayama, and H. Takayanagi, *Phys. Rev. B* **73**, 161303(R) (2006).
- [18] J. Bork, Y.-H. Zhang, L. Diekhöner, L. Borda, P. Simon, J. Kroha, P. Wahl, and K. Kern, *Nat. Phys.* **7**, 901 (2011).
- [19] Q. Yang, L. Wang, Z. Zhou, L. Wang, Y. Zhang, S. Zhao, G. Dong, Y. Cheng, T. Min, Z. Hu, W. Chen, K. Xia, and M. Liu, *Nat. Commun.* **9**, 991 (2018).
- [20] H. Imamura, P. Bruno, and Y. Utsumi, *Phys. Rev. B* **69**, 121303(R) (2004).
- [21] A. Schulz, A. DeMartino, P. Ingenhoven, and R. Egger, *Phys. Rev. B* **79**, 205432 (2009).
- [22] H.-R. Chang, J. Zhou, S.-X. Wang, W.-Y. Shan, and D. Xiao, *Phys. Rev. B* **92**, 241103(R) (2015).
- [23] J. Gao, W. Chen, X. C. Xie, and F. C. Zhang, *Phys. Rev. B* **80**, 241302(R) (2009).
- [24] Q. Liu, C.-X. Liu, C. Xu, X.-L. Qi, and S.-C. Zhang, *Phys. Rev. Lett.* **102**, 156603 (2009).
- [25] G. Yang, C.-H. Hsu, P. Stano, J. Klinovaja, and D. Loss, *Phys. Rev. B* **93**, 075301 (2016).
- [26] C.-H. Hsu, P. Stano, J. Klinovaja, and D. Loss, *Phys. Rev. B* **96**, 081405(R) (2017).
- [27] C.-H. Hsu, P. Stano, J. Klinovaja, and D. Loss, *Phys. Rev. B* **97**, 125432 (2018).
- [28] J. Sinova, S. O. Valenzuela, J. Wunderlich, C. H. Back, and T. Jungwirth, *Rev. Mod. Phys.* **87**, 1213 (2015); M. Z. Hasan and C. L. Kane, *ibid.* **82**, 3045 (2010).
- [29] M. Zare, F. Parhizgar, and R. Asgari, *Phys. Rev. B* **94**, 045443 (2016).
- [30] F. D. M. Haldane, *Phys. Rev. Lett.* **61**, 2015 (1988).
- [31] C. L. Kane and E. J. Mele, *Phys. Rev. Lett.* **95**, 226801 (2005).
- [32] B. A. Bernevig, T. L. Hughes, and S.-C. Zhang, *Science* **314**, 1757 (2006).
- [33] M. Ezawa, *Phys. Rev. Lett.* **110**, 026603 (2013).
- [34] S. Konschuh, M. Gmitra, and J. Fabian, *Phys. Rev. B* **82**, 245412 (2010).
- [35] G. Usaj, P. M. Perez-Piskunow, L. E. F. Foa Torres, and C. A. Balseiro, *Phys. Rev. B* **90**, 115423 (2014).
- [36] A. Kundu, H. A. Fertig, and B. Seradjeh, *Phys. Rev. Lett.* **113**, 236803 (2014).
- [37] T. J. Huisman, R. V. Mikhaylovskiy, J. D. Costa, F. Freimuth, E. Paz, J. Ventura, P. P. Freitas, S. Blgel, Y. Mokrousov, T. Rasing *et al.*, *Nat. Nanotechnol.* **11**, 455 (2015); T. Seifert, S. Jaiswal, U. Martens, J. Hannegan, L. Braun, P. Maldonado, F. Freimuth, A. Kronenberg, J. Henrizi, I. Radu *et al.*, *Nat. Photon.* **10**, 483 (2016).
- [38] M. Sherafati and S. Satpathy, *Phys. Rev. B* **83**, 165425 (2011).
- [39] A. M. Black-Schaffer, *Phys. Rev. B* **81**, 205416 (2010).
- [40] See Supplemental Material at <http://link.aps.org/supplemental/10.1103/PhysRevB.99.121409> for details on (a) the square lattice model, (b) analytical treatment and properties of the Green's function and (c) dependence on the strength of the spin-orbit coupling.
- [41] This can be understood by the fact that for the second-order process, the connecting states need to traverse the whole perimeter irrespective of the positions of the spins.
- [42] C. W. J. Beenakker and H. van Houten, *Solid State Phys.* **44**, 1 (1991).
- [43] Instead of the integral over the full bandwidth below the Fermi energy in Eq. (2), in practical systems, a finite mean free path (i.e., a finite lifetime of the states) of the electron would result in a much smaller effective range of the integral. Moreover, the bulk states of QSH are not protected against backscattering, so one expects a much shorter mean free path of the bulk states compared to the edge states.
- [44] P. Stano, J. Klinovaja, A. Yacoby, and D. Loss, *Phys. Rev. B* **88**, 045441 (2013).
- [45] D. F. Kirwan, C. G. Rocha, A. T. Costa, and M. S. Ferreira, *Phys. Rev. B* **77**, 085432 (2008); E. J. G. Santos, A. Ayuela, S. B. Fagan, J. Mendes Filho, D. L. Azevedo, A. G. Souza Filho, and D. Sánchez-Portal, *ibid.* **78**, 195420 (2008); S. R. Power, V. M. de Menezes, S. B. Fagan, and M. S. Ferreira, *ibid.* **80**, 235424 (2009); I. C. Gerber, A. V. Krasheninnikov, A. S. Foster, and R. M. Nieminen, *New J. Phys.* **12**, 113021 (2010).
- [46] A. M. Black-Schaffer, *Phys. Rev. B* **82**, 073409 (2010).